GRAPHITIZATION OF PBO FIBRE CHARS AS SEEN BY X-RAY SCATTERING AND HRTEM

M.B. Vázquez-Santos[1], Amelia Martínez-Alonso[1], J.M.D. Tascón[1], J.-N. Rouzaud[2], E. Geissler[3], K. László[4]*

[1] Instituto Nacional del Carbón, CSIC, Apartado 73, 33080 Oviedo, Spain,[2] Laboratoire de Géologie de l'Ecole Normale Supérieure, UMR CNRS 8538, 24 rue Lhomond, 75231 Paris Cedex 5, France,[3]Laboratoire de Spectrométrie Physique, UMR CNRS 5588. Université Joseph Fourier de Grenoble, BP 87, 38402 Saint Martin d'Hères cedex, France,[4] Department of Physical Chemistry and Materials Science, Budapest University of Technology and Economics, H-1521 Budapest, Hungary.

Introduction

Poly(*p*-phenylene benzobisoxazole) (PBO) is a rigid-rod polymer with outstanding mechanical and thermal properties, having the highest tensile modulus, tensile strength, and thermal stability among commercial polymeric fibres [1].

Pyrolysis of PBO fibres at 700-1000 ºC yields chars with limited ultramicroporosity [2]. PBO, like many conventional non-melting polymers, yields chars that contain a limited amount of ultramicropores and are easy to activate physically [3]. PBO-derived carbon fibres (CFs) heat-treated at temperatures up to 2400 ºC do not display the interlayer spacing of graphite, but the CFs are more ordered than those prepared from conventional feedstock polymers [4]. PBO-derived fibres heat-treated up to 3000 ºC, however, transform into graphitized carbon [5]. Here we investigate the structural and microtextural changes in PBO-derived carbon fibres that occur as a function of heat treatment temperature *T* (900°C≤*T*≤ 2700°C), using small- and wide-angle X-ray scattering (SAXS and WAXS, respectively) as well as high-resolution transmission electron microscopy (HRTEM).

Experimental

PBO (Zylon®, Toyobo, Japan) fibres were pyrolyzed for 1 h at 900 ºC in a tubular quartz reactor under argon flow. Portions of the carbonized material were taken for further treatment at higher temperatures in a graphite furnace, also under argon flow for 1 h. The samples are denoted T900, T1600, T2000, T2400 and T2700. X-ray scattering measurements were made on the fibres at the BM2 beam line at the ESRF, Grenoble, France, in the wave vector range $2.5\times10^{-2}\leq q\leq 50$ nm^{-1}. TEM observations were made on a Jeol 2011 microscope equipped with a LaB6 gun working at 200 kV. The samples were finely ground and dispersed in ethanol, and a drop of the solution was deposited on a standard TEM copper grid, covered by a lacey amorphous carbon film. Bright-field (BF) techniques were employed. In some cases, the images were coupled to selected area electron diffraction (SAED) for structural analyses of a volume smaller than 1 µm in diameter and 0.1 µm in thickness. The 002 lattice fringe ("high-resolution") mode, with magnifications up to 500,000×, was used to image the profile of the aromatic layers and hence the structure and the microtexture.

Results and Discussion

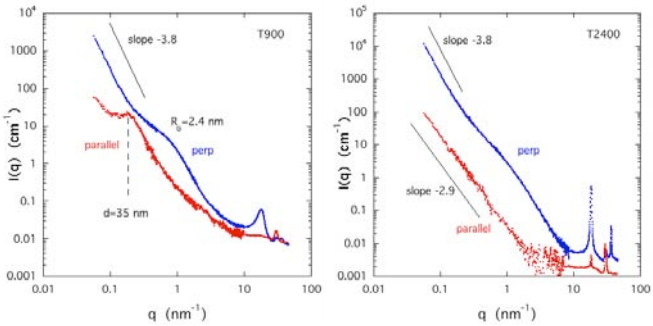

Fig. 1 : X-ray scattering responses in perpendicular and parallel directions. a: T900, b: T2400

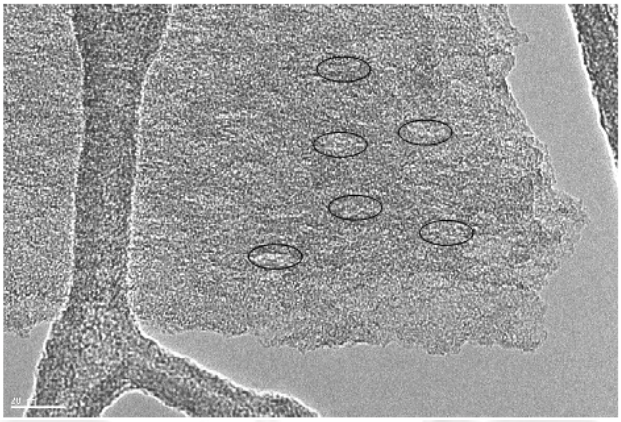

Fig. 2 : T900. BF image. Scale bar 20 nm. Elongated pores (black ellipses) oriented along (horizontal) fibre axis.

Fig. 3 T2000. Scale bar 5 nm. 002 lattice fringe image showing coherent domain growth. The layers forming a pore wall are larger and more planar and the microtexture tends to be lamellar. Some fringes remain normal to the orientation.

Figs. 1 a,b show the projections of the X-ray scattering intensity $I(q)$ along the directions parallel and perpendicular to the fibre axis for two values of preparation temperature *T*. $I(q)$ evolves with increasing *T*, both in the SAXS (q < 10 nm^{-1}) and in the WAXS regions (10 nm^{-1} < q < 50 nm^{-1}). In the direction parallel to the fibre axis, the SAXS intensity is lower than in the perpendicular direction, as expected from long rods. The

anisotropy in T900 implies that this property is inherited from the parent PBO fibre [1]. The SAXS response reflects the mutual arrangement of the component fibrils, but the overall radius of the fibres is much larger than the largest value of $2\pi/q$ explored here. In the lowest q-region of Fig. 1, the scattering response perpendicular to the fibre axis displays a power law, the slope of which is intermediate between -3 and -4, which is the signature of rough interfaces within the fibres. This feature is absent in the parallel direction, which means that the interfaces lie parallel to the fibre axis, i.e., the fibril stacks are oriented approximately parallel to the draw axis of the fibre. In the parallel direction at low q a resolved peak appears, corresponding to weakly correlated features with a characteristic spacing $2\pi/q \approx 35$ nm. This scattering is due to pores, detected by bright field TEM (black ellipses in **Fig. 2**).

The HRTEM micrographs in **Figs 2 - 4** show a high degree of order (preferential orientation of the layers parallel to the fibre axis), with local structural defects progressively removed during the thermal treatment. Fig. 2 exhibits graphitic layer stacks with thickness (2-3 nm) that are consistent with the shoulder feature in Fig. 1. At high T (> 2000°C), the HRTEM images show the transition from fibrous to lamellar microtexture. Such a transition is required for the development of the AB stacking of graphene layers, characteristic of the graphite order; such structural evolution was confirmed by SAED. **Fig. 5** shows how, w ith increasing *T*, the (002, 100, 101, 004, 103) reflections sharpen and approach the values corresponding to graphite.

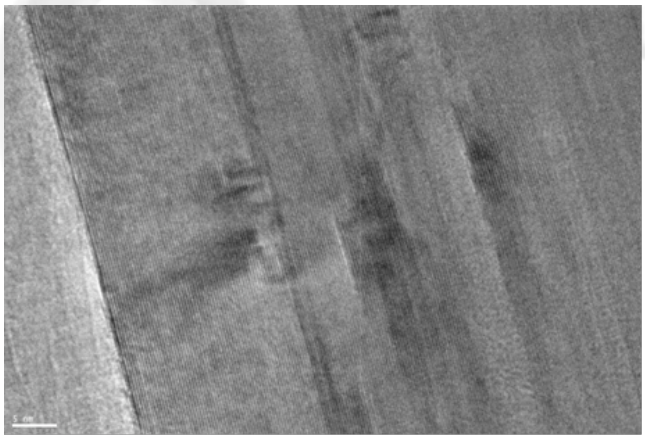

Fig. 4. T2700. 002 lattice fringe image showing graphite lamellae: perfect stacking of very large layers. Scale bar 5 nm.

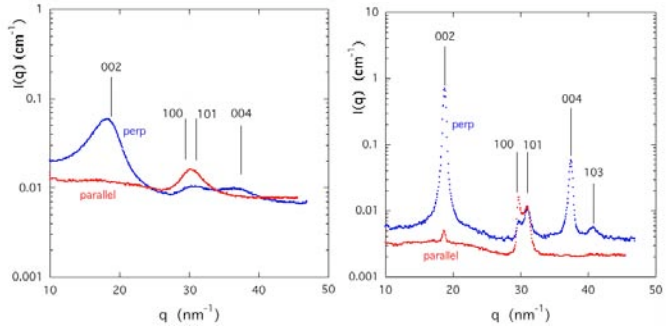

Fig. 5: Evolution with *T* of the scattering spectra in the WAXS region; a: T900, b: T2700. Vertical lines denote positions of the Bragg peaks of graphite, with their corresponding indices.

Conclusions

Graphitisation of carbon fibres derived from PBO under different temperatures of heat-treatment follows a mechanism that differs from the standard route of graphitisable carbons as found in anthracene-based cokes [6]. A similar mode of graphitization has been reported by Oberlin and coworkers in polyimide films [7,8]. The deformation introduced by drawing the fibre preferentially aligns the polymer crystallites, thereby determining a preferential orientation of the graphene sheets parallely to the draw fibre axis. This microtextural feature governs both the internal fibril structure (i.e., the polyaromatic Basic Structural Units) in the carbonised fibre and then, with increasing T, the subsequent formation of the graphite crystallites. The HRTEM images of the graphene sheets profile reveal defects of orientation that are consistent with the angular spread of the SAXS intensity around its maximum, perpendicular to the fibre axis. Heat treatment causes disappearance of pores and, consequently, the occurrence of a lamellar microtexture. This allows the subsequent graphitization, but does not reduce the larger-scale misorientation of the crystallites.

Acknowledgments. The authors are grateful to the ESRF, Grenoble, for access to the French CRG beamline BM2 and to the Laboratoire de Réactivité de Surface, Université Pierre et Marie Curie, Paris, for access to the Jeol 2011 TEM. Financial support from the Hungary-Spain Integrated Actions Programme (ESP-3/2006 and HH2006-0026) and from the CSIC - Hungarian Academy of Sciences cooperation is gratefully acknowledged. M.B.V.S. acknowledges receipt of a JAE grant from the Spanish CSIC.

References

[1] Chae HG, Kumar S. Rigid-rod polymeric fibres. J Appl Polym Sci 2005; 100 (1):791–802.

[2] Vázquez-Santos MB, Martínez-Alonso A, Tascón JMD. Porosity development in chars from termal degradation of poly (*p*-phenylene benzobisoxazole). Polym Degrad Stab 2009;94(1):7-12.

[3] Vázquez-Santos MB, Martínez-Alonso A, Tascón JMD. Activated carbon fibers from poly(*p*-phenylene benzobisoxazole). Carbon 2008;46(5)825-8.

[4] Newell JA, Edie DD, Fuller ELJr. Kinetics of carbonization and graphitization of PBO fiber. J Appl Poym Sci 1996;60(6):825-32.

[5] Kaburagi Y, Yokoi K, Yoshida A, Hishiyama Y. Highly graphitized carbon fiber prepared from poly(*p*-phenylene benzobisoxazole) fiber. Tanso 2005;[No. 217]:111-4.

[6] Rouzaud JN, Oberlin A. Structure, microtexture, and optical-properties of anthracene and saccharose-based carbons. Carbon 1989;27(4):517–29.

[7] Guigon M, Oberlin A, Desarmot G. Microtexture and structure of some high-tensile strength, PAN-base carbon-fibers. Fibre Sci Technol 1984;20(1):55-72.

[8] Inagaki M, Takeichi T, Hishiyama Y, Oberlin A. High quality graphite films produced from aromatic polyimides. In: Thrower PA, Radovic LR, editors. Chemistry and physics of carbon, vol. 26, New York: Dekker; 1999 p. 245-333.